Multi-analyte homogenous immunoassay based on quenching of quantum dots by functionalized graphene

ANALYTICAL AND BIOANALYTICAL CHEMISTRY, 406 (2014), 4841-4849

DOI: 10.1007/s00216-014-7885-6

MULTI-ANALYTE HOMOGENOUS IMMUNOASSAY BASED ON QUENCHING OF QUANTUM DOTS BY FUNCTIONALIZED GRAPHENE

L. Anfossi[1]*, P. Calza[1], F. Sordello[1], C. Giovannoli[1], F. Di Nardo[1], C. Passini[1], M.Cerruti[2], I.Y. Goryacheva[3], E.S. Speranskaya[3], C. Baggiani[1]

[1] Department of Chemistry, University of Turin. Via Giuria, 5, I-10125 Turin, Italy

[2] Materials Engineering, McGill University, 3610 University St., Montreal, QC H3A 0C5, Canada

[3] Department of General and Inorganic Chemistry, Chemistry Institute, Saratov State University, Astrakhanskaya 83, 410012 Saratov, Russia

*to whom correspondence should be addressed. Tel: +390116705219, fax: +390116705242. E-mail: laura.anfossi@unito.it

Abstract

We propose a homogenous multi-analyte immunoassay based on the quenching of quantum dot (QD) fluorescence by means of graphene. Two QDs with emission maxima at 636 and 607 nm were bound to antibodies selective for mouse or chicken immunoglobulins, respectively, and graphene functionalized with carboxylic moieties was employed to covalently link the respective antigen. The antibody-antigen interaction led graphene close enough to QDs to quench the QD fluorescence by resonance energy transfer. The addition of free antigens that competed with those linked to graphene acted as a “turn on” effect on QD fluorescence. Fluorescence emitted by the two QDs could be recorded simultaneously since the QDs emitted light at different wavelengths while being excited at the same, and proved to be linearly correlated with free antigen concentration. The developed assay allows measuring both antigens over two-three orders of magnitude and showed estimated limits of detection in the nanomolar range. This approach is thus a promising universal strategy to develop homogenous immunoassays for diverse antigens (cells, proteins, low-molecular-mass analytes) in a multi-analyte configuration.

Keywords: immunoassay, antibody, homogeneous assay, quantum dot, graphene, resonance energy transfer, fluorescence quenching

Introduction

Quantum dots (QDs) are fluorescent semiconductor nanocrystals with extremely high quantum yields, narrow and tunable emission spectra, wide excitation range, high resistance to photobleaching, and simultaneous excitation of multiple fluorescence colors [1,2]. These exceptional optical properties make

QDs very attractive in a number of applications including solar cells [3], LED screens [4] and, recently, labels for biosensing of analytes including DNA, proteins, cells, and small organic molecules [2,5-7]. QDs are typically core/shell inorganic particles with sizes comprised between 2 and 10 nm, often covered with hydrophilic polymeric films for water compatibility and bioconjugation. When acting as biolabels, QDs have been mostly used as donors in biosensors based on the Förster resonance energy transfer (FRET) mechanism [5,8-9]; however, there are also a few examples of QDs used as fluorescent labels for the development of highly-sensitive [10-12], multi-analyte immunoassays [13-15].

Just a few years ago, Quian and co-workers showed a simple and elegant fluoroimmunoassay based on the optical properties of QDs and the fluorescence quenching ability of graphene [5]. In this sandwich immunoassay the capture antibody was covalently linked to hydrothermally converted graphene sheets and the reporter antibody was labelled with a QD. Adding the antigen to a solution containing both antibodies gave rise to the formation of a two-site immunocomplex that led the QDs close enough to graphene to determine the transfer of energy and fluorescence quenching, and thus acted as a “turn off” input on QD emission. The quenching efficiency depended on the antigen concentration and was independent over a wide range of distances (tens to one hundred nanometers) between the donor (QD) and the quencher (graphene).

In the wake of this pioneering work, Chen and co-workers designed another competitive homogenous immunoassay exploiting the QD-graphene energy transfer, however with a “turn on” model. In this case, QD-labelled antibodies directly interacted with graphene oxide sheets via π-π stacking and hydrogen bonding. If a large antigen such as a human virus bound to the antibody, the distance between the QD and the graphene oxide sheet increased enough to suppress the energy transfer between the QD and graphene oxide, and the QD luminescence was turned on [2]. This “turn on” model showed a higher efficiency and lower background than the “turn off” model. In addition, authors proved the multi-analyte detection potential of their strategy, by using QDs that could be excited at the same excitation wavelength and emitted differently colored fluorescence signals to simultaneously detect two human viruses. Nevertheless, the use of different antibodies by other authors did not give the same results shown by Chen and co-workers [16], and this assay format was limited to the detection of very large antigens, such as cells and pathogens.

Based on Chen’s work, Quian et al very recently described a more general fluoroimmunoassay design based on the energy transfer between QD-loaded graphene (QDGNP) and graphene (GNP) [16]. Antibodies are linked to the QDGNP donor through the QD portion of the ensemble, and the proximity between QDGNP and GNP is guaranteed by π-π interactions between GNP and QDGNP sheets. This is a “turn on” assay, where the QD luminescence is turned on when an immunocomplex forms between the labelled antibody and its macromolecular antigen (human IgG), thus pushing QDGNP away from GNP [16]. Although

this strategy does not require the antibody to interact with GNP via π-π stacking, which limited the type of antibodies that could be used in Chen's assay [2], it is still constrained by antigen nature and dimension.

In a previous work, we functionalized graphene with carboxylate groups on GNP (GNP-COOH) that could act as shape controller i.e. towards TiO_2 nanoplates [17-18]. We propose here an approach to develop a homogenous fluoroimmunoassay based on QD-labelled antibodies and functionalized graphene (GNP-COOH) covalently linked to the antigen as the QD fluorescence quencher. The assay is designed as a competitive immunoassay, in which the free antigen, i.e. the analytical target, and the GNP-linked antigen compete for binding to the QD-labelled antibody. The displacement of GNP-linked antigen from the immunocomplex due to competition with the free antigen determines the restoration of QD luminescence. Therefore, the free antigen determines and modules a "turn on" effect on QD fluorescence emission, as schematically illustrated in Figure 1. The surface modification of GNP [19-23] allows us to covalently conjugate antigens to the quencher thus bringing the QD-labelled antibody close enough to the GNP to permit energy transfer. We show that it is possible to simultaneously determine the concentration of two antigens by using antibodies labelled with QDs that differ in emitted light colour while being excited at the same wavelength. This strategy can be regarded as a truly universal approach, since different antigens (cells, proteins, and small molecules) can be covalently bound to GNP-COOH via a very straightforward conjugation chemistry based on carbodiimide coupling.

Materials and methods

Chemicals

Polyclonal antibodies towards chicken immunoglobulins (Ab_{vs}CIg) developed in rabbit and towards mouse immunoglobulins (Ab_{vs}MIg) developed in goat, *N*-(3-Dimethylaminopropyl)-*N*'-ethylcarbodiimide hydrochloride (EDAC), bovine serum albumin fraction V (BSA), cadmium oxide (CdO, 99,99%), selenium powder (Se, 99,99%), sulfur powder (S, 99%), zinc acetate ($Zn(OAc)_2$, 99,99%), oleic acid (OA, 90%), 1-octadecene (ODE, 90%), oleylamine (OLA, 70%), octadecylamine (ODA, 90%), poly(maleic anhydride-alt-1-octadecene) (PMAO, M ~ 30 000-50 000), rhodamine 6G, 4–aminophenylacetic acid, and HCl sodium nitrite were purchased from Sigma-Aldrich (MO, USA). Mouse and chicken immunoglubulins were the fraction obtained from the respective animal serum through sulfate ammonium precipitation. Jeffamine M1000 (1000 g/mol) was kindly provided by Huntsman (Belgium). Black well microplates and all other chemicals were obtained from VWR International (PA, USA). Phosphate buffer saline (PBS, phosphate20mM, pH 7.4) was used as the diluent for the homogenous assays.

Graphene nanopowder functionalization

Graphene nanopowder (GNP, Graphene Supermarket, 3 nm flakes, Grade AO1) was modified with carboxylic groups using diazonium chemistry [18-19]. To prepare this sample, from now on called GNP-

106 COOH, the GNP powder was added to a solution containing 0.05 M 4–aminophenylacetic acid, 0.5 M HCl
107 and 0.05 M sodium nitrite. The reaction was carried out for ten minutes; then GNP-COOH was filtered
108 (Whatman cellulose acetate filter with 3.0 µm pores) and washed several times with deionized (DI) water
109 and isopropyl alcohol, and let dry overnight at 323 K. A complete characterization of the synthetized
110 material is reported elsewhere [17]).
111
112 *QD synthesis*
113 Hydrophilic core/shell/shell CdSe/CdS/ZnS QDs with emission at 636 nm (QDI) and at 607 nm (QDII)
114 and photoluminescence quantum yield ~30% were synthesized. First CdSe QDs with two different
115 diameters (4.4 nm and 3.7 nm) were prepared by a hot-injection method described in [24-26]. The
116 diameters of the QDs were determined on basis of the calibration curve from [27]. Then CdSe QDs were
117 covered with 3 layers of CdS and 2 layers of ZnS by SILAR (Successive Ionic Layer Adsorption and Reaction)
118 method [28, 29]. The solutions of precursors for shell growth were prepared as follows. The Cd precursor
119 solution (0.05 M) was prepared by combining CdO, oleic acid (molar ratio CdO:OA was 1:8) with ODE inside
120 a three-neck flask and heating at 210°C under argon atmosphere until the solution turned clear. The S
121 precursor solution (0.05 M) was made by dissolving S in ODE at 160 °C under argon. The Zn precursor
122 solution (0.05 M) was prepared in a glovebox by dissolving zinc acetate in a mixture of oleylamine and
123 octadecene (v(Zn)/v(OLA)=1:8) at 120 °C. For a typical synthesis 20 ml of ODE and 4.5 g of ODA were loaded
124 into a 100 ml reaction flask and heated at 100 °C under argon for 1 hour. About 3×10^{-4} mmol of CdSe core
125 nanocrystals in hexane was added to the flask and the mixture was flushed with argon for 1 hour to remove
126 the hexane. Then the flask was heated up to 225 °C. The S and Cd (or Zn) precursor solutions (0.05 M) were
127 added consecutively via syringe to the reaction flask containing the CdSe cores, waiting 10 min after each
128 injection. This was followed by alternating addition of Cd or Zn precursors and S precursor, respectively. We
129 determined the amount of the injection solution by method [27] based on the calculation of the number of
130 surface atoms. Upon completion of the synthesis, the reaction was cooled down to ~70 °C and small
131 amount of chloroform was added to prevent solidification of amine. Then the clear solution was transferred
132 to a centrifugation tube and acetone was added until opalescence appeared. The mixture was centrifuged
133 for 7 min at 2700 g. Afterwards the precipitate was dissolved in toluene and stored in a refrigerator under
134 Ar.
135 To transfer QDs to aqueous solution, we prepared the amphiphilic polymer (poly(maleic anhydride-
136 alt-1-octadecene) – Jeffamine M1000, PMAO-PEG): 2 g of Jeffamine M1000 was dissolved in 15 ml
137 chloroform and was added drop by drop to a flask containing 1 g of PMAO. The powder immediately
138 dissolved and the solution was refluxed at 60°C during 1 hour under nitrogen and then was left under
139 stirring overnight. Purified QDs and the amphiphilic polymer were mixed in chloroform and stirred
140 overnight at room temperature (mass ratio of QD:PMAO was ~1:7). An equal volume of KOH solution (0.05

141 M) was added to the QDs-polymer chloroform solution. Afterwards the chloroform was slowly evaporated
142 by a Bunsen's water-air-jet pump and a clear fluorescent solution was obtained. To remove the polymer
143 excess, chloroform was added drop by drop to QDs aqueous solution (V($CHCl_3$):V(QDs solution)=1:1). As a
144 result, a white precipitate at the chloroform-water interface was formed. The sample was centrifuged at
145 2700 g and the aqueous phase was taken away. The procedure was repeated 3-4 times until the next
146 chloroform addition did not provoke the formation of any visible white precipitate. After that the solution
147 was placed under reduced pressure (with water-jet pump) to remove chloroform residues. Excess of
148 Jeffamine M1000 was removed by three rounds of ultrafiltration with Amicon centrifuge filters (100kD
149 MWCO).
150 For the estimation of quantum yield (QY), the spectrally integrated emission of quantum dot
151 solutions were compared to the emission of dyes with known quantum yield (6 G: QY=95% at λ (exc.)=490
152 nm) as described in [30].
153
154 *Preparation of QD-antibody conjugates*
155 We prepared QDI-Ab_{vs}MIg and QDII-Ab_{vs}CIg as follows. 0.1 ml of QDs diluted in 1 ml of PBS were pre-
156 activated with 0.05 ml of a freshly prepared aqueous solution of EDAC (10 mg/ml) for 20 min at room
157 temperature. Then, we added 0.5 mg of Ab_{vs}MIg or Ab_{vs}CIg to the pre-activated QDI and QDII, respectively,
158 and incubated for 30 min at room temperature. A second aliquot of EDAC was added and the tubes were
159 transferred to 4°C for a further overnight incubation. To ensure the complete covering of QD surface with
160 proteins, we used 1 mg of BSA (0.1 ml of a 10 mg/ml PBS solution) to end-cap QD-antibody conjugates and
161 these were stored at 4°C until use QD-antibody conjugates were characterized by recording emission
162 spectra on a CARY Eclipse fluorescence spectrophotometer (Agilent Technologies, CA, USA) before and
163 after conjugation. QD-labeled antibodies were separated from unbound antibodies by ultracentrifugation
164 at 16000 x g for 30 min.
165
166 *Preparation of GNP-protein conjugates*
167 GNP-COOH was reacted with both mouse and chicken immunoglobulins to prepare the GNP-COOH-
168 MIg-CIg conjugate. Briefly, 1 mg of GNP-COOH was dispersed in 0.4 ml of PBS by sonicating for 15 min, and
169 then activated by adding EDAC as described above. 0.5 mg of each immunoglobulin was then added and
170 incubated for 30 min at room temperature. A second EDAC aliquot was then added, the mixture was
171 incubated overnight at 4°C, and 1 mg of BSA was added to end-cap the GNP-MIg-CIig conjugate. The GNP
172 end product was recovered by centrifugation at 3000 x g for 5 min. The pellet was washed twice with PBS
173 and finally recovered in 1 ml of PBS. The suspension was sonicated for 15 min, diluted 1:100 with PBS and
174 stored at 4°C until use. We estimated the rate of immunoglobulins (either MIg or CIg) conjugated to GNP-

175 COOH by measuring immunoglobulins remaining in the supernatant, which proved to be undetectable.
176 Therefore, immunoglobulins were completely bound to GNP-COOH.
177
178 *Inhibition of QD fluorescence due to interaction with GNP-COOH-MIg-CIg*
179 The interaction between GNP-COOH-MIg-CIg and QD-antibody conjugates was evaluated by
180 recording the fluorescence emission on a FLx800 fluorescence microplate reader (BioTek, VT, USA). The
181 excitation and emission wavelengths were set at 360 (±40) nm and 460 (±40) nm, respectively.
182 Checkerboard titrations were adopted to establish amounts of QD-Ab_{vs}MIg or QD-Ab_{vs}CIg and GNP-COOH-
183 MIg-CIg. 10, 20, and 40 µl of QDI-Ab_{vs}MIg or QDII-Ab_{vs}CIg were mixed with 10 µl of the GNP-COOH-MIg-CIg
184 conjugate previously diluted at 1:10, 1:100, and 1:1000. PBS was added to reach an overall volume of 200
185 µl. The fluorescence quenching due to the interaction between GNPGNP-COOH-MIg-CIg and QD-$_{vs}$MIg or
186 QD_{vs}CIg was observed between 10' and 90'. The emission of QD-Ab_{vs}MIg or QD-Ab_{vs}CIg alone and mixed
187 with GNP-COOH were measured too, to check for non-specific binding and other non-specific causes of
188 fluorescence decay.
189
190 *Homogeneous assays based on QD fluorescence quenching by GNP*
191 To check the efficacy of the competitive assay, we first tested a model including only a single analyte.
192 We put in contact different amounts of either antigen (MIg or CIg) with fixed amounts of the QD
193 functionalized with the corresponding antibody in the presence of the GNP-COOH-MIg-CIg. More
194 specifically, 40 µl of QDI-Ab_{vs}MIg or 20 µl QDII-Ab_{vs}CIg were mixed in the wells of a microplate reader with
195 10 µl of GNP-COOH-MIg-CIg (diluted 1:100) and with 100 µl of either MIg or CIg (0-1.5-7.5-30-100-500
196 mg/l), respectively. PBS was added to reach an overall volume of 200 µl, and the mixture was incubated for
197 30' at room temperature. The emitted fluorescence was then recorded as indicated above.
198 To assess the possibility of establish a multi-analyte assay, based on the unique optical property of
199 QDs that can be excited at the same wavelength and emit light at different wavelengths, experiments were
200 conducted by employing the same protocol, except that all volumes were doubled and QDI-Ab_{vs}MIg**,** QDII-
201 Ab_{vs}CIg, GNP-COOH-MIg-CIg and both antigens were all mixed together. Fluorescence was recorded on the
202 CARY Eclipse fluorescence spectrophotometer, with excitation wavelength of 350 nm, and emission
203 recorded between 550 and 680 nm.
204 Standard curves were obtained by plotting fluorescence emitted at 594 nm against CIg concentration
205 and fluorescence emitted at 634 nm against MIg concentration, based on the emission maxima of QDI and
206 QDII, respectively. Curves obtained by subtracting the signal of the blank (no target protein in the sample)
207 to the signals of solutions containing different protein amounts were fitted by a 4-parameter logistic
208 equation.
209

210 **Results and Discussion**

211 The multianalyte "turn on" fluoroimmunoassay that we propose is based on the competitive binding
212 of free antigens and QD-labelled antigens on GNP on which we have immobilized CIg and MIg. The binding
213 between CIg and MIg on GNP is mediated by COOH groups covalently bound to GNP using diazonium
214 chemistry (Figure 2). Briefly, carboxylate groups are added to GNP starting from 4–aminophenylacetic acid
215 as precursor, as previously described by Sordello et al [17] (Figure 2a). The carboxylate groups then react
216 with amino groups present in CIg and MIg with mediation of EDAC, and a covalent amide bond is formed
217 between CIg and MIg and GNP at the end of the process (Figure 2b).

218 Successful conjugation between QDs and antibodies is shown by the changes in QD emission spectra
219 (Figure 3): when excited at 230 nm, unmodified QDI and QDII show emission maxima at 636 nm and 607
220 nm, respectively (Figures 3 a and b, continuous line spectra); after conjugation with antibodies (Figure 3 a
221 and b, dashed lines), a further emission band shows up at about 330 nm for both QDs, which is attributable
222 to the fluorescence of the covalently bound antibodies [31]. Nevertheless, the second harmonic of
223 fluorescence due to antibodies interfered with QD emission. To avoid this interference, we set the
224 excitation wavelength at 350 nm (Figures 3 c and d). In these conditions, only the contribute to
225 fluorescence due to QDs was observed and emission maxima of QD conjugated to antibodies (dashed lines)
226 were observed at 634 and 594 nm for QDI and QDII, respectively . A further less intense emission was also
227 observed at about 440 nm for both QDs when conjugate to antibodies and excited at 350 nm.

228 The conjugation with antibodies should yield QDs able to selectively bind the corresponding antigen
229 present on GNP, thus bringing the QDs and the GNP close enough to allow for energy transfer and
230 quenching of QD fluorescence. We studied the interaction between QD-Ab_{vs}MIg and QD-Ab_{vs}CIg and GNP-
231 COOH-MIg-CIg by measuring QD fluorescence as a function of the QD/GNP ratio and contact time (Figure
232 4). As control samples, we use bare QDs in interaction with GNP-COOH-MIg-CIg, as well as QD-Ab_{vs}MIg and
233 QD-Ab_{vs}CIg alone. All the results are summarized in Table 1, and Figure 4 shows those obtained for QD-
234 Ab_{vs}MIg as an example. When QDs and functionalized GNP are mixed, the fluorescence decreases almost
235 linearly as a function of time. The combination of conjugated QDs and GNP-COOH-MIg-CIg yielded a more
236 evident fluorescence decrease, which depended on GNP-COOH-MIg-CIg amount (namely on QD-Ab/ GNP-
237 COOH-MIg-CIg ratio): GNP-COOH-MIg-CIg diluted 1:100 was the most effective in inducing fluorescence
238 quenching, followed by the 1:10 dilution. The 1:1000 dilution showed a slower decay in QD emission,
239 however significantly different from that observed for the control systems. We expected a lower efficiency
240 in fluorescence quenching when decreasing the amount of GNP-COOH-MIg-CIg, however, the 1:10 dilution
241 showed less quenching than the 1:100 dilution. We hypothesize that higher GNP-COOH-MIg-CIg
242 concentrations lead to less stable suspensions or to the establishment of interactions within GNP-COOH-
243 MIg-CIg sheets, which reduce their availability for binding to conjugated QDs.

Control samples show a much lower decrease in fluorescence when unconjugated QDs are mixed with GNP-COOH-MIg-CIg (Figure 4 a-c, grey symbols), and an almost constant fluorescence emission for both conjugated and unconjugated QDs in the absence of GNP-COOH-MIg-CIg, except for a minor decrease in the first 30 minutes (Figure 4d). This indicates that some non-specific interactions between QDs and GNP may occur, which cause a delayed reduction of QD emission. Nevertheless, the faster fluorescence reduction observed for the QD-Ab_{vs}MIg and QD-Ab_{vs}CIg when mixed with GNP-COOH-MIg-CIg systems proves the establishment of the antibody-antigen binding.

Homogeneous immunoassay for a single analyte

After showing that the binding of QDs conjugated to antibodies to functionalized GNP does indeed quench QD fluorescence, we can proceed to test the homogeneous competitive immunoassay described above (Figure 1). The closeness of QDs to GPN, due to the binding between antibodies linked to QDs and their antigens linked to GPN sheets, determined a strong quenching of the QD fluorescence, therefore a homogenous competitive immunoassay could be designed, based on the inhibition of QD/GPN binding in the presence of the antigen in the same solution (Figure 1). The addition of increasing amounts of antigens to the QD-Ab_{vs}MIg and QD-Ab_{vs}CIg /GNP-COOH-MIg-CIg mixture should cause a parallel increase in QD fluorescence, since the QDs conjugated to antibodies should bind to the free antigen and be displaced from GNP-COOH-MIg-CIg.

We defined the optimal conditions for the homogenous competitive immunoassay using a standard checkerboard assay, in which we selected the appropriate competitor concentrations (i.e. the amount of functionalized GNP) and antibody dilutions (i.e. the amount of QD conjugated to antibodies) based on the lowest IC_{50}. We ran these tests as microplate assays, separately on QDI/MIg and QDII/CIg systems. We optimized the incubation time by comparing dose-response curves obtained after 30, 60 or 90 min of reaction. We also checked the possibility of cross-reaction within the two systems, i.e. the possibility that QDI-Ab_{vs}MIg could bind to CIg and *vice-versa*. The results are summarized in Figure 5, which shows typical inhibition curves for the two systems obtained by plotting fluorescence against concentrations of the target antigens and non-specific antigens at different incubation times. Figure 5a shows inhibition curves obtained by mixing QDI-Ab_{vs}MIg and the functionalized GNP with increasing amounts of MIg (solid symbols), which represented the target antigen, and with CIg (open symbols) to assess cross-reactivity, while Figure 5b shows inhibition curves obtained for QDII-Ab_{vs}CIg, in the presence of its target analyte (CIg, open symbols) and with the potentially cross-reagent MIg (solid symbols). Both systems proved to respond to the presence and quantity of their respective antigen, as expected, whereas cross-reactivity between the two targets resulted negligible in all cases. Based on these results, we selected 30 min incubation as a satisfactory compromise between the lowest IC_{50} and data precision.

Multi-analyte homogenous assay

After showing that our competitive assay can measure the presence of one analyte in solution, we tested the possibility of using it to determine two analytes at the same time by measuring fluorescence at two wavelengths. We mixed together the two QDs conjugated to antibodies (QDI-Ab_{vs}MIg , QDII-Ab_{vs}CIg), GNP-COOH-MIg-CIg and the two target antigens (MIg and CIg) and incubated the mixture for 30 min at room temperature. Then we measured the fluorescence emitted between 550 and 680 nm, using an excitation wavelength of 350 nm. The increment of each antigen in the mixture induced the increase of the emitted fluorescence at the expected wavelength (Figure 6). A partial overlap of emission was observed, due to the fact that QDI and QDII have close emission maxima (594 and 634 nm). Nevertheless, calibration curves for the two targets could be obtained by plotting fluorescence values (arbitrary units) measured at 634 and 594 nm against MIg and CIg concentrations, respectively (Figure 7). The developed assay allows measuring both antigens in a wide concentration interval (two-three orders of magnitude) and showed estimated limits of detection in the nanomolar range.

Conclusions

We developed a competitive homogenous immunoassay, based on labelling antibodies with quantum dots and exploiting the quenching of QD fluorescence by resonance energy transfer to graphene. We functionalized graphene with carboxylic groups (GNP-COOH), which allowed for covalent linking of antigens to graphene sheets. The establishment of the antibody-antigen interaction brings QD and graphene close enough to permit the energy transfer and, thus, the quenching of QD fluorescence. The competition between free and graphene-linked antigens causes the displacement of QD-labelled antibodies form graphene.The presence of free antigens thus restores QD fluorescence, acting as a “turn on” input. The emitted light is linearly related to the free antigen amount. This method is universal, i.e. it potentially can work with analytes of any molecular weight provided that they can be covalently linked to GNP-COOH through its carboxylic functional groups, differently from previously reported methods [2,5]. The detection itself is fast enough as the assay is fully homogeneous, whereas heterogeneous immunoassays involve multiple steps of incubation. The stability of the fluorescence of conjugated QDs in the absence of related antigens allows using their fluorescence intensity as an internal calibration standard, thus simplifying result analysis. Finally, the proposed strategy is applicable in a multi-analyte configuration.

Acknowledgements

We acknowledge support from a Marie Curie International Research Staff Exchange Scheme Fellowship (PHOTOMAT, proposal n° 318899) within the 7th European Community Framework Programme, and from the Canada Research Chair foundation.

314

315 **References**

316 [1] Durán GM, Contento AM, Ríos Á (2013) Use of Cdse/ZnS quantum dots for sensitive detection and
317 quantification of paraquat in water samples, Anal Chim Acta 801 84– 90
318 [2] Chen L, Zhang X, Zhou G, Xiang X, Ji X, Zheng Z, He Z, Wang H (2012) Simultaneous Determination of
319 Human Enterovirus 71 and Coxsackievirus B3 by Dual-Color Quantum Dots and Homogeneous
320 Immunoassay. Anal Chem 84: 3200−07
321 [3] Kamat PV (2013) Quantum Dot Solar Cells. The Next Big Thing in Photovoltaics . Phys Chem Lett 4 (6):
322 908-918
323 [4] Bae WK, Kwak J, Lim J, Lee D, Nam MK, Char K, Lee C, Lee S (2010) Multicolored light-emitting diodes
324 based on all-quantum-dot multilayer films using layer-by-layer assembly method Nano Lett10(7):2368-73
325 [5] Liu M, Zhao H, Quian X, Chen S, Fan X (2010) Distance-independent quenching of quantum dots by
326 nanoscale-graphene in self-assembled sandwich immunoassay Chem Commun 46: 7909–11
327 [6] Dong et al., Fluorescence Resonance Energy Transfer between Quantum Dots and Graphene Oxide for
328 Sensing Biomolecules Anal. Chem., 2010, 82: 5511–5517
329 [7] Wang et al., Graphene and graphene oxide: biofunctionalization and applications in biotechnology,
330 Trends in Biotechnol., 2011, 5: 205–212.
331 [8]Algar WR, Krull UJ (2008) Quantum dots as donors in fluorescence resonance energy transfer for the
332 bioanalysis of nucleic acids, proteins, and other biological molecules. Anal Bioanal Chem 391(5):1609-18.
333 [9] Medintz IL, Mattoussi H (2009) Quantum dot-based resonance energy transfer and its growing
334 application in biology Phys Chem Chem Phys 11(1):17-45
335 [10] Zekavati R, Safi S, Hashemi SJ, Rahmani-Cherati T, Tabatabaei M, Mohsenifar A, Bayat M (2013) Highly
336 sensitive FRET-based fluorescence immunoassay for aflatoxin B1 using cadmium telluride quantum dots
337 Microchimica Acta 180 (13-14):1217-23
338 [11]Kim J, Kwon S, Park JK, Park I (2014) Quantum dot-based immunoassay enhanced by high-density
339 vertical ZnO nanowire array. Biosens Bioelectron 55:209-15
340 [12] He Y, Tian J, Hu K, Zhang J, Chen S, Jiang Y, Zhao Y, Zhao S (2013)An ultrasensitive quantum dots
341 fluorescent polarization immunoassay based on the antibody modified Au nanoparticles amplifying for the
342 detection of adenosine triphosphate. Anal Chim Acta 802:67-73.
343 [13] Beloglazova N., Speranskaya E., De Saeger S., et al. (2012) Quantum dot based rapid tests for
344 zearalenone detection. Anal Bioanal Chem 403: 3013-24
345 [14] Yu W, Kim IS, Niessner R, Knopp D (2012) Multiplex competitive microbead-based flow cytometric
346 immunoassay using quantum dot fluorescent labels. Anal Chim Acta 750:191-8.
347 [15] Zeng Q, Zhang Y, Liu X, Tu L, Kong X, Zhang H (2012) Multiple homogeneous immunoassays based on a
348 quantum dots-gold nanorods FRET nanoplatform. Chem Commun (Camb) 48(12):1781-3.

[16] Zhao H, Chang Y, Liu M, Gao S, Yu H, Quan X (2013) A universal immunosensing strategy based on regulation of the interaction between graphene and graphene quantum dots, Chem Commun, 49: 234-36

[17] Sordello F, Zeb G, Hu K, Calza P, Minero C, Szkopek T, Cerruti M, Tuning TiO_2 nanoparticle morphology in graphene–TiO_2 hybrids by graphene surface modification, Nanoscale, DOI: 10.1039/C4NR01322K

[18] Zeb G, Gaskell P, Le X T, Xiao X, Szkopek T, Cerruti M (2012) Decoration of graphitic surfaces with Sn nanoparticles through surface functionalization using diazonium chemistry. Langmuir 28: 13042-50.

[19] Peng C, Xiong Y, Liu Z, Zhang F, Ou E, Qian J, Xiong Y, Xu W (2013) Bulk functionalization of graphene using diazonium compounds and amide reaction. Appl Surf Sci 280: 914-919

[20] Lee S W, Kim, BS, Chen S, Shao-Horn Y, Hammond P T (2008) Layer-by-Layer Assembly of All Carbon Nanotube Ultrathin Films for Electrochemical Applications. Am Chem Soc 131 (2): 671-679

[21] Lyskawa J, Bélanger D (2006) Direct Modification of a Gold Electrode with Aminophenyl Groups by Electrochemical Reduction of in Situ Generated Aminophenyl Monodiazonium Cations. Chem Mater 18 (20): 4755-4763

[22] Pinson J, Podvorica F (2005) Attachment of organic layers to conductive or semiconductive surfaces by reduction of diazonium salts. Chem Soc Rev 34 (5): 429-439

[23] Mahouche-Chergui S, Gam-Derouich S, Mangeney C, Chehimi M M (2011) Aryl diazonium salts: a new class of coupling agents for bonding polymers, biomacromolecules and nanoparticles to surfaces. Chem. Soc. Rev., 40 (7): 4143-66

[24] Jasieniak J, Bullen C, van Embden J, Mulvaney P (2005) Phosphine-free synthesis of CdSe nanocrystals. J Phys Chem B 109 (44):20665–68.

[25] Capek R K, Moreels I, Lambert K, De Muynck D, Zhao Q, Van Tomme A, Vanhaecke F, Hens Z. Optical Properties of Zincblende Cadmium Selenide Quantum Dots. J Phys Chem C (2010) 114 (14): 6371–76.

[26] Beloglazova NV, Shmelin PS, Speranskaya ES, Lucas B, Helmbrecht C, Knopp D, Niessner R, De Saeger S, Goryacheva I.Yu. (2013) Quantum Dot Loaded Liposomes As Fluorescent Labels for Immunoassay. Anal Chem 85: 7197–7204

[27]Yu WW, Qu L, Guo W, Peng X (2003) Experimental determination of the extinction coefficient of CdTe, CdSe, and CdS Nanocrystals. Chem Mater 15:2854–60.

[28] Reiss P, Protière M, Liang L Core/Shell Semiconductor Nanocrystals Small (2009) 5(2): 154–168.

[29] Li J J, Wang, Y A, Guo W Z, Keay J C, Mishima TD, Johnson M B, Peng X G (2003) Large-Scale Synthesis of Nearly Monodisperse CdSe/CdS Core/Shell Nanocrystals Using Air-Stable Reagents via Successive Ion Layer Adsorption and Reaction. J Am Chem Soc 125: 12567-75

[30] Grabolle M, Spieles M, Lesnyak V, Gaponik N, Eychmuller A, Resch-Genger U (2009) Determination of the Fluorescence Quantum Yield of Quantum Dots: Suitable Procedures and Achievable Uncertainties. Anal Chem 81: 6285–6294.

383 [31] Eftink M R (2000) Intrinsic Fluorescence of Proteins Topics in Fluorescence Spectroscopy. Topics in
384 Fluorescence Spectroscopy 6:1-15
385

386 **TABLES**

387 Table 1. Linear fit of QD fluorescence decay due to the interaction between QD conjugated to
388 antibodies (QDI-Ab_{vs}MIg and QDII-Ab_{vs}CIg) and GNP functionalized with the corresponding antigen as a
389 function of time of contact for various GNP-COOH-MIg-CIg amounts. As a control quenching of non-
390 conjugated QDs (QDI and QDII) was also evaluated.

391

	GNP-COOH-MIg-CIg dilution		
	1:10	**1:100**	**1:1000**
QDI	y=-1.23x+246, r^2=0.968	y=-1.02x+287, r^2=0.926	y=-1.18x+170, r^2=0.962
QDI-Ab_{vs}MIg	y=-1.74x+246, r^2=0.992	y=-2.03x+294, r^2=0.997	y=-1.51x+229, r^2=0.995
QDII	y=-1.39x+297, r^2=0.983	y=-1.13x+342, r^2=0.967	y=-1.21x+206, r^2=0.974
QDII-Ab_{vs}CIg	y=-1.55x+277, r^2=0.983	y=-2.07x+190, r^2=0.998	y=-1.53x+194, r^2=0.993

392

393

394 **FIGURES**

395

396 **Figure 1**. Schematic of the multi-analyte homogeneous immunoassay based on fluorescence
397 quenching of two QDs conjugated with antibodies by means of GNP-COOH covalently linked to
398 corresponding antigens**.** Mouse Immunoglobulins (MIg) and Chicken Immunoglobulins (CIg) are coupled to
399 GNP-COOH and interact with 2 QDs labeled with antibodies developed towards MIg and CIg respectively
400 (1). When light is shined on this configuration, no fluorescence is observed because the QD fluorescence is
401 quenched by GNP (2). The addition of antigens, one at a time (3-4) or mixed together (5), restores
402 fluorescence of the respective QD.

403

404 **Figure 2.** GNP functionalization to yield GNP-COOH (a) and its covalent modification to prepare GNP-
405 COOH-MIg-Cig (b)

406

407 **Figure 3.** Emission spectra of QD before (continuous lines) and after conjugation (dashed lines) with
408 antibodies: excitation was set at 230 nm (a and b) or 350 nm (c and d)

409

410 **Figure 4.** Quenching of QDII fluorescence due to the interaction between unconjugated QD (grey
411 symbols, ■) or QD conjugated to antibodies (black symbols,◆) and GNP functionalized with the
412 corresponding antigen as a function of time of contact and for various functionalized GNP amounts (a-c). As
413 a further control, QD and QD-Ab_{vs}CIg were also incubated in the absence of functionalized GNP (d).

414

415 **Figure 5**. Inhibition of binding of conjugated QDs to GNP-COOH-MIg-CIg by MIg (solid symbols) or CIg
416 (open symbols) added to the solution after increasing incubation times: 30' (●), 60' (■), and 90' (▼). QDI-
417 Ab_{vs}MIg (a) and QDII-Ab_{vs}CIg (b) were separately incubated with increasing amounts of each of the two
418 antigens and the emitted fluorescence was measured by means of a fluorescence microplate reader
419 (excitation: 360±40 nm, emission: 460±40 nm).

420

421 **Figure 6.** Emission spectra recorded by means of a fluorescence spectrophotometer (excitation 350
422 nm) for the multi-analyte system. QDI-Ab_{vs}MIg and QDII-Ab_{vs}CIg were mixed with the GNP-COOH-MIg-CIg
423 and target analytes at two concentration levels: 0 (solid line) and 500 mg l^{-1} (dashed line).

424

425 **Figure 7**. Typical calibration curves obtained in the multi-analyte assay configuration by plotting
426 fluorescence emitted at 594 nm (●) and 634 nm (■) against CIg and MIg concentrations, respectively.
427 Measured fluorescence (arbitrary units) in the absence of any targets (FU_0) was subtracted to the
428 fluorescence measured at each individual target concentration. Inset shows actual measured fluorescence.

429 FIGURES

430 Figure 1

431
432
433
434

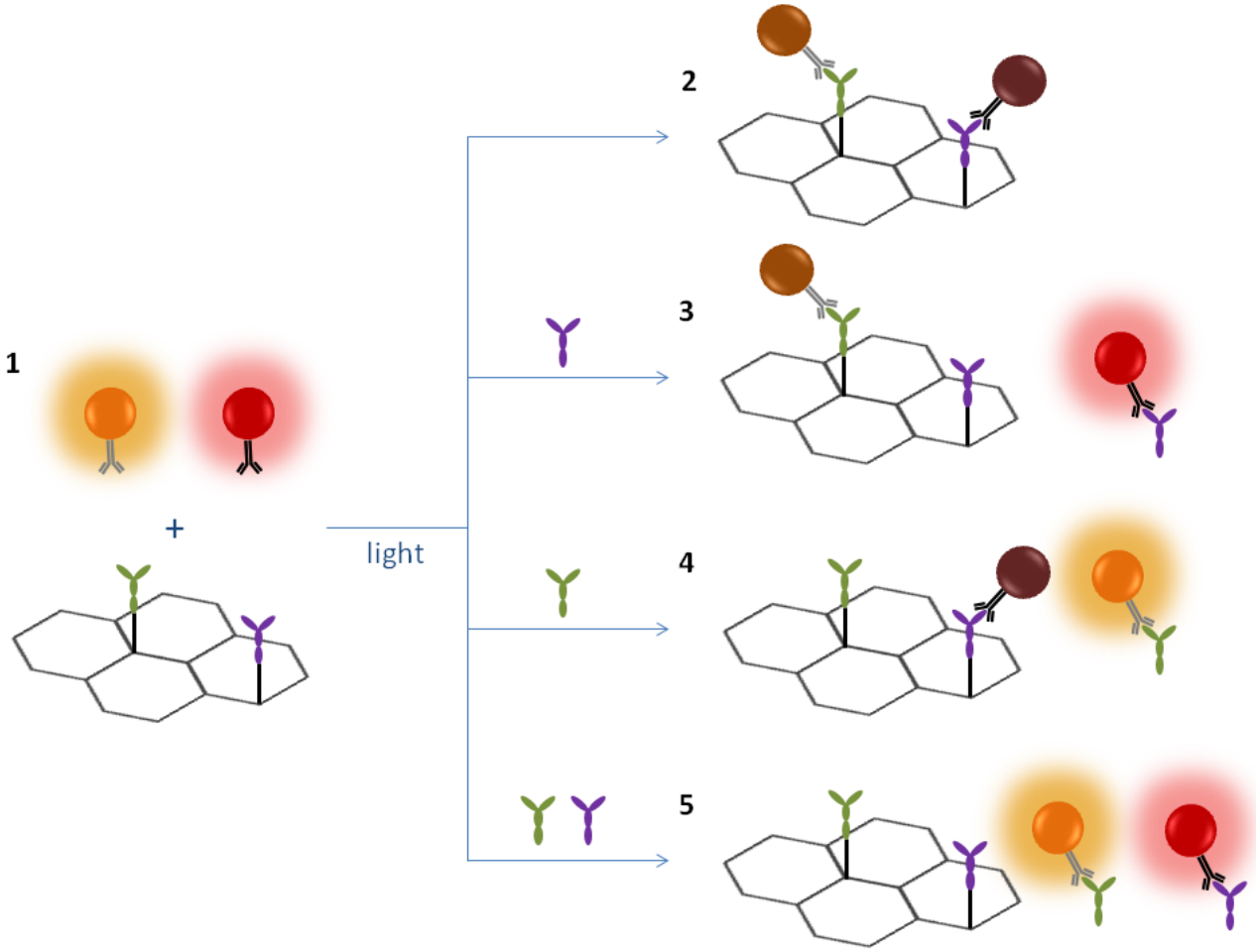

435
436

437 Figure 2
438
439

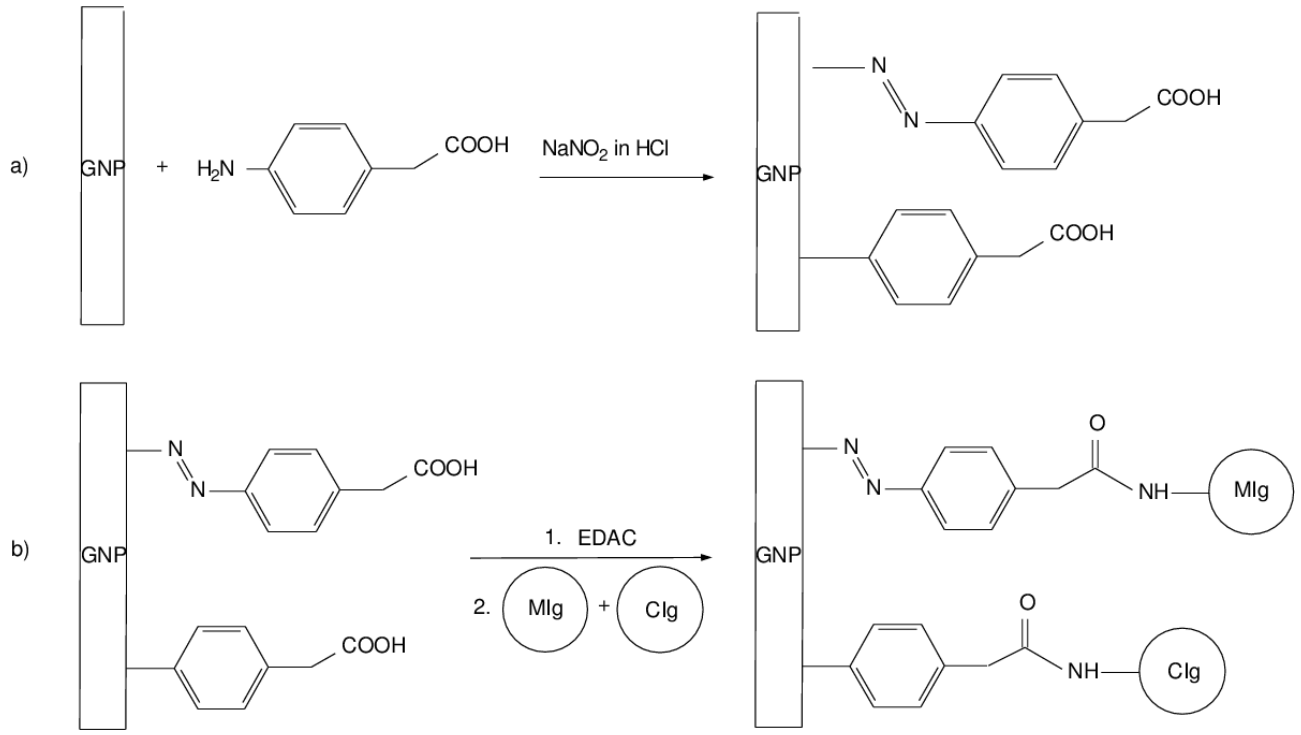

440
441

Figure 3

a

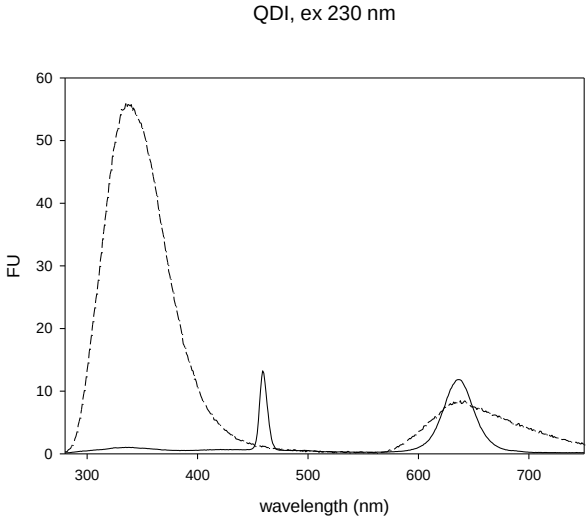

b

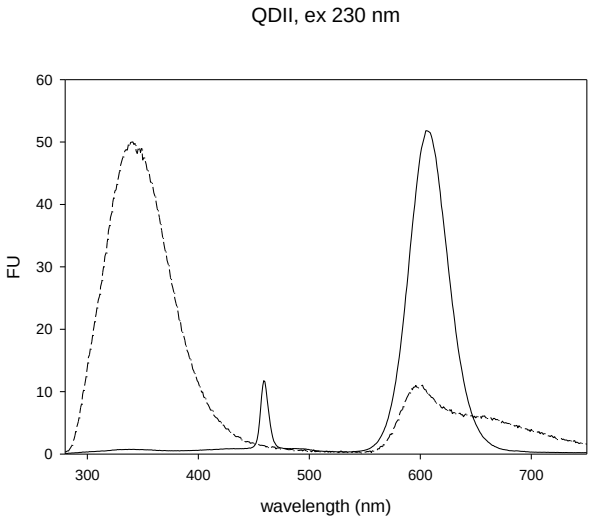

c

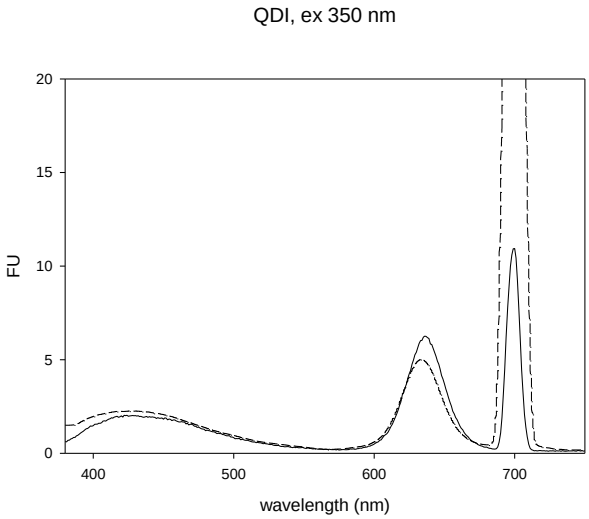

d

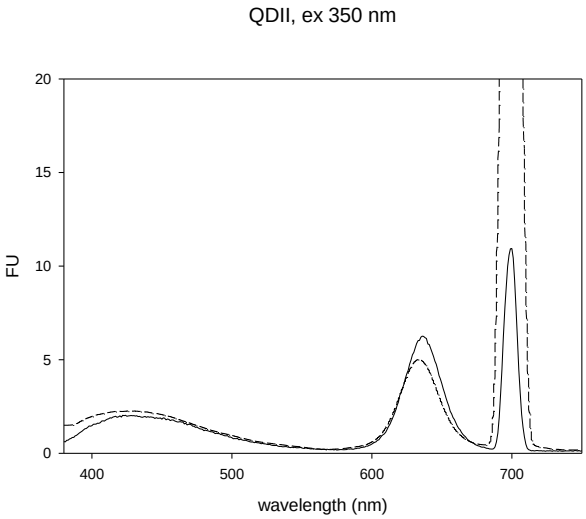

Figure 4

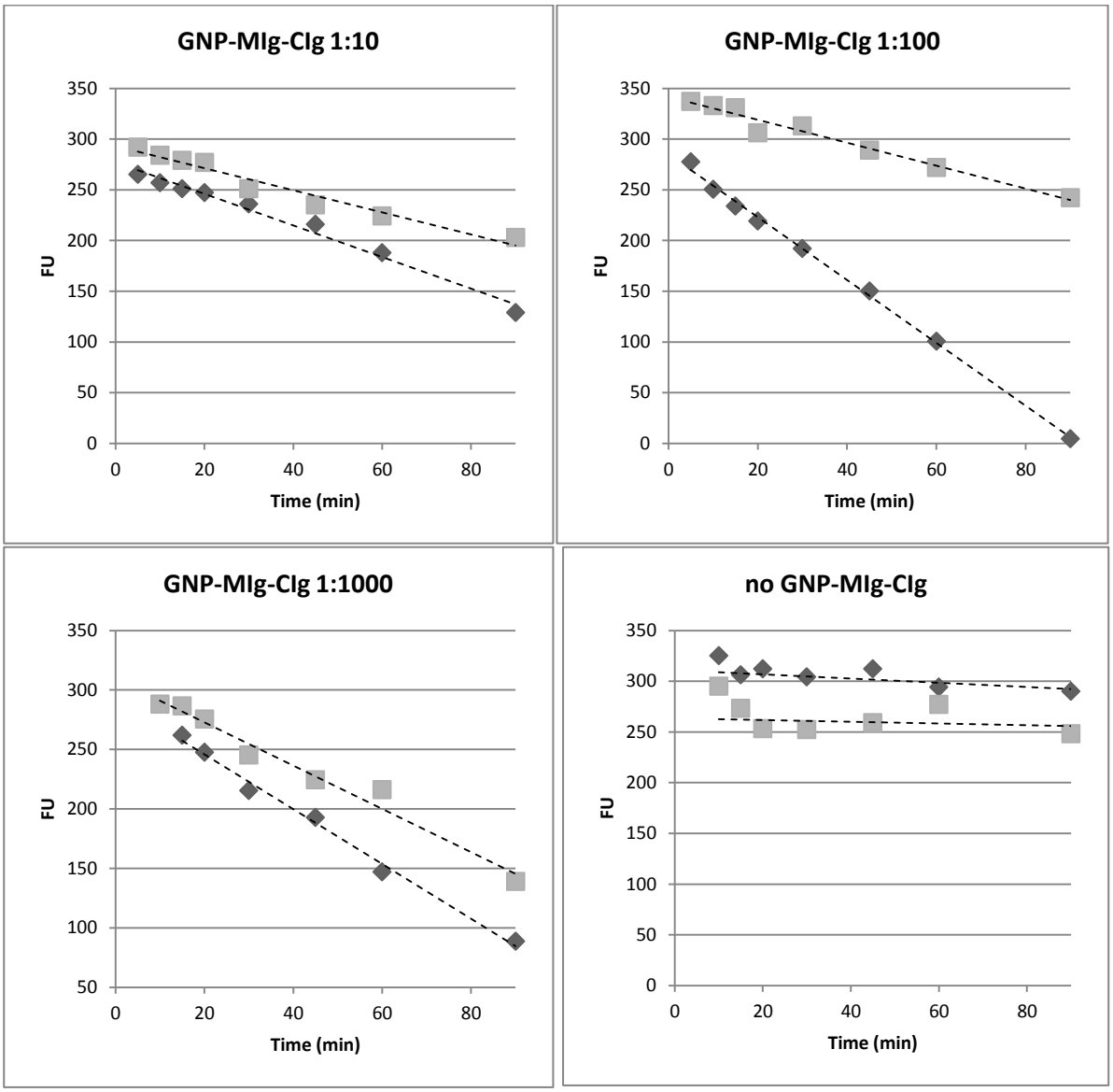
GNP-MIg-CIg 1:10
GNP-MIg-CIg 1:100
GNP-MIg-CIg 1:1000
no GNP-MIg-CIg
FU
Time (min)
0
50
100
150
200
250
300
350
0
20
40
60
80

Figure 5

a

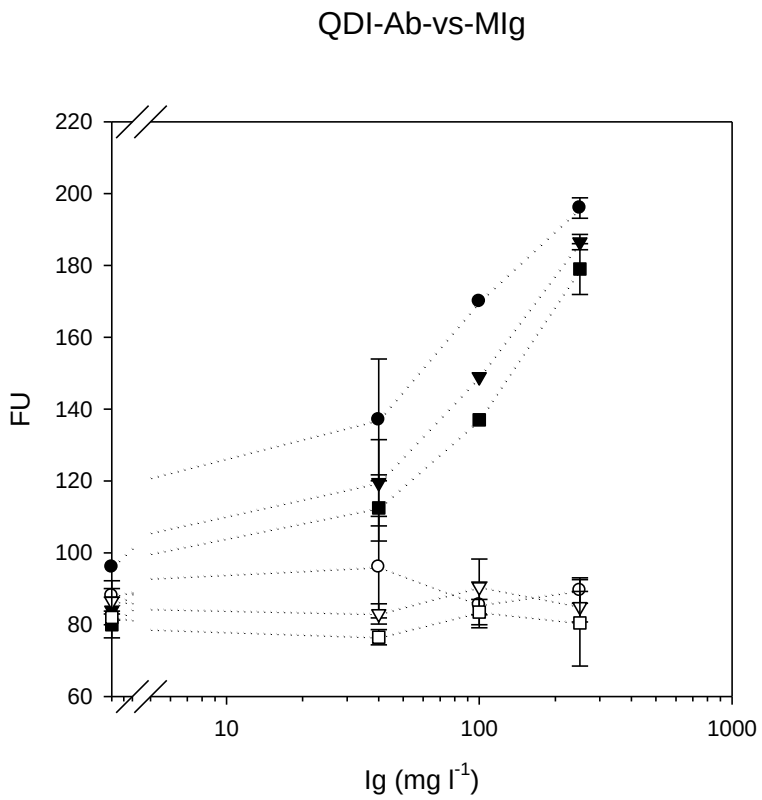
QDI-Ab-vs-MIg
FU
220
200
180
160
140
120
100
80
60
10
100
1000
Ig (mg l-1)

b

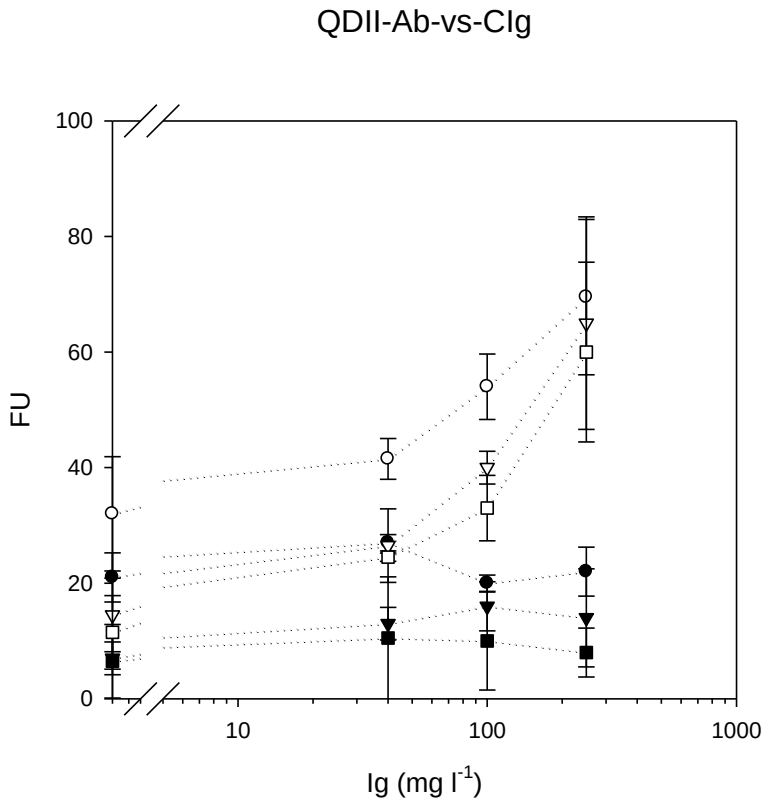
QDII-Ab-vs-CIg
FU
100
80
60
40
20
0
10
100
1000
Ig (mg l-1)

Figure 6

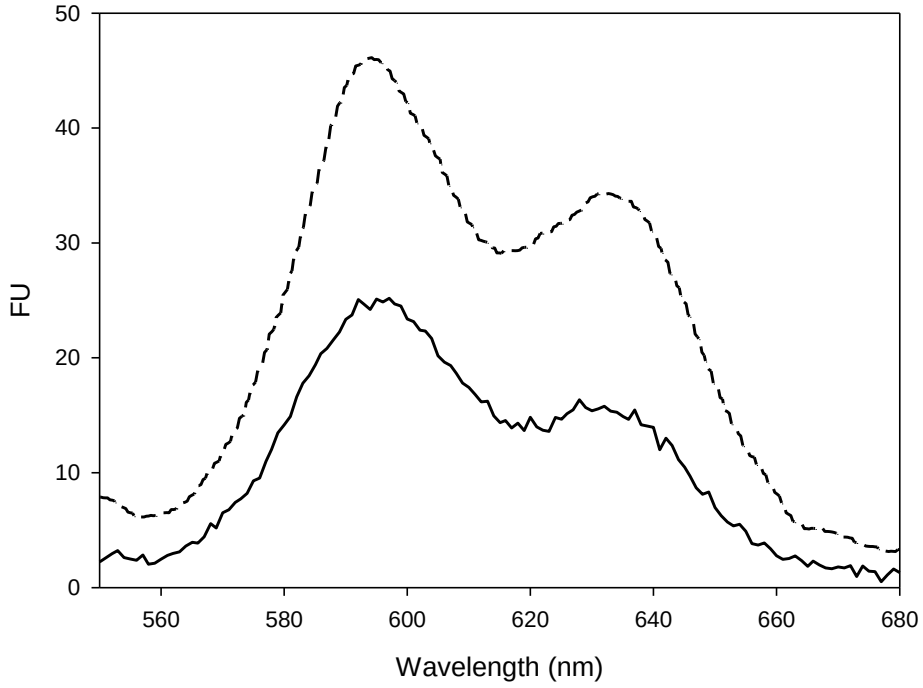

Figure 7

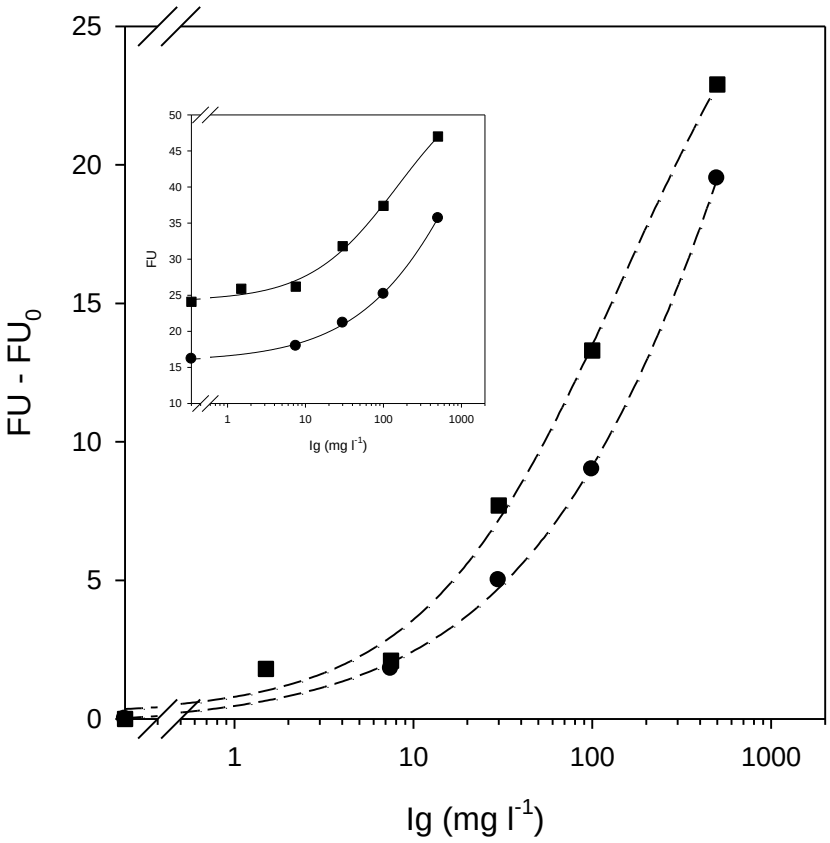
25
20
15
10
5
0
FU - FU0
1
10
100
1000
Ig (mg l-1)
50
45
40
35
30
25
20
15
10
FU
1
10
100
1000
Ig (mg l-1)